Preclinical evaluation of trabectedin in combination with targeted Inhibitors for treatment of metastatic uveal melanoma

Glinkina, K.; Nemati, F.; Teunisse, A.F.A.S.; Gelmi, M.C.; Etienne, V.; Kuipers, M.J.; ... ; Jochemsen, A.G.

Preclinical Evaluation of Trabectedin in Combination With Targeted Inhibitors for Treatment of Metastatic Uveal Melanoma

Kseniya Glinkina,[1] Fariba Nemati,[2] Amina F. A. S. Teunisse,[1] Maria Chiara Gelmi,[3] Vesnie Etienne,[2] Muriel J. Kuipers,[1] Samar Alsafadi,[4] Martine J. Jager,[3] Didier Decaudin,[2,5] and Aart G. Jochemsen[1]

[1]Department of Cell and Chemical Biology, Leiden University Medical Center, Leiden, The Netherlands
[2]Laboratory of Preclinical Investigation, Department of Translational Research, Institut Curie, PSL University, Paris, France
[3]Department of Ophthalmology, Leiden University Medical Center, Leiden, The Netherlands
[4]Uveal Melanoma Translational Group, Department of Translational Research, Institut Curie, PSL University, Paris, France
[5]Department of Medical Oncology, Institut Curie, PSL University, Paris, France

Correspondence: Aart G. Jochemsen, Department of Cell and Chemical Biology, Leiden University Medical Center, Postbus 9600, 2300 RC Leiden, The Netherlands; a.g.jochemsen@lumc.nl.

Received: October 5, 2022
Accepted: November 21, 2022
Published: December 14, 2022

Citation: Glinkina K, Nemati F, Teunisse AFAS, et al. Preclinical evaluation of trabectedin in combination with targeted inhibitors for treatment of metastatic uveal melanoma. *Invest Ophthalmol Vis Sci.* 2022;63(13):14. https://doi.org/10.1167/iovs.63.13.14

Purpose. Uveal melanoma (UM) is considered a rare disease; yet, it is the most common intraocular malignancy in adults. Although the primary tumor may be efficiently managed, more than 50% of patients with UM develop distant metastases. The mortality at the first year after diagnosis of metastatic UM has been estimated at 81%, and the poor prognosis has not improved in the past years due to the lack of effective therapies.

Methods. In order to search for novel therapeutic possibilities for metastatic UM, we performed a small-scale screen of targeted drug combinations. We verified the targets of the tested compounds by western blotting and PCR and clarified the mechanism of action of the selected combinations by caspase 3 and 7 activity assay and flow cytometry. The best two combinations were tested in a mouse patient-derived xenograft (PDX) UM model as putative therapeutics for metastatic UM.

Results. Combinations of the multitarget drug trabectedin with either the CK2/CLK double-inhibitor CX-4945 (silmitasertib) or the c-MET/TAM (TYRO3, Axl, MERTK) receptor inhibitors foretinib and cabozantinib demonstrated synergistic effects and induced apoptosis (relative caspase 3 and 7 activity increased up to 20.5-fold in UM cell lines). In the case of the combination of foretinib and cabozantinib, inhibition of the TAM receptors, but not c-Met, was essential to inhibit the growth of UM cells. Monotreatment with trabectedin inhibited tumor growth by 42%, 49%, and 35% in the MM26, MM309, and MM339 PDX mouse models, respectively.

Conclusions. Trabectedin alone or in combination with cabozantinib inhibited tumor growth in PDX UM mouse models. Blocking of MERTK, rather than TYRO3, activity inhibited UM cell growth and synergized with trabectedin.

Keywords: metastases, uveal melanoma, trabectedin, MERTK

Uveal melanoma (UM) is a malignant tumor that arises from the melanocytes located in the uveal tract of the eye. Uveal melanoma is considered a rare disease, with an incidence of two to eight cases per million per year in Europe[1]; yet, it is the most common intraocular malignancy in adults. Although the primary tumor may be efficiently managed by the local therapy, more than 50% of patients with UM develop distant metastases. UM metastases are in most cases restricted to the liver; other metastatic sites are the lungs, skin, brain, thyroid, and colon.[2] Metastatic UM is very aggressive, as the mortality at the first year after diagnosis reaches 81%.[3]

The poor prognosis for patients with metastatic UM has not improved in the past years due to the lack of effective novel therapies. One established local treatment option for hepatic metastases is isolated liver perfusion with the chemotherapeutic agent melphalan. The response rate to this therapy is reported to be higher than 50%, with significant regression of the lesions. However only a restricted cohort of patients is eligible, the recurrence of metastases after the isolated liver perfusion is frequent, and the procedure is complex and potentially associated with morbidity.[4–7]

Numerous recently conducted clinical trials for metastatic UM have resulted in limited improvement in overall survival.[8] Among the drugs tested are chemotherapeutics such as dacarbazine (alone or in combination with the mitogen-activated protein kinase kinase [MEK] inhibitor selumetinib) and fotemustine,[9,10] as well as some targeted therapeutics such as the MEK inhibitor trametinib,[11] the

Table 1. Drugs Included in the Screen

Drug	Target/Mechanism of Action	Clinical Trials Phase	References
Trabectedin	RNA Pol II, DNA-bound proteins, tumor microenvironment/ multitarget DNA-damaging agent	III	Monk et al.[36]
CX-4945	Casein kinase 2, Cdc2-like kinases	Ib/II	Borad et al.[37]
Foretinib	C-MET, VEGFR2, TAM (TYRO, Axl, MERTK) receptors	II	Rayson et al.[38]
RG7112	MDM2–p53 interaction/p53 activator	I	Andreeff et al.[39]

Table 2. Uveal Melanoma Cell Lines Included in the Screen

Cell Line	Origin	GNAQ Mutation	GNA11 Mutation	BAP1 Expression
OMM2.3	Liver metastasis	c.626 A>C	—	Yes
OMM2.5	Liver metastasis	c.626 A>C	—	Yes
OMM1	Subcutaneous metastasis	—	c.626 A>T	Yes
MM66	PDX established from liver metastasis	—	c.626 A>T	Yes
MM28	PDX established from liver metastasis	—	c.626 A>T	No
MP46	PDX established from primary tumor	c.626 A>T	—	No
MP38	Primary tumor	c.626 A>T	—	No

tyrosine kinase inhibitor imatinib,[12] and the heat shock protein 90 (HSP90) inhibitor ganetespib.[13] Immunotherapeutic targeting of programmed death protein 1 (PD-1), recognized as a promising option for metastatic cutaneous melanoma, has demonstrated no effect on overall survival of the patients with metastatic UM, with the exception of UM with the methyl-binding domain protein 4 (MBD4) mutation and increased mutation load.[14,15] At present, the only approved systemic treatment is tebentafusp, a bispecific protein able to bind simultaneously to the glycoprotein 100 (gp100)–human leukocyte antigen (HLA)-A*02:01 complex on UM cells and cluster of differentiation 3 (CD3) on the T-cell membrane, thus redirecting the T cells toward UM cells. The phase III trial of tebentafusp in patients with HLA-A*02:01–positive metastatic UM delivered encouraging results. Overall survival at 1 year was 73% in the treatment group and 59% in the control group, and progression-free survival also increased significantly.[16]

Commonly, UM has a relatively low mutation burden.[17,18] The most recurrent alterations (more than 90% of all cases) are activating mutations in the genes *GNAQ* or *GNA11* encoding the G-proteins Gαq and Gα11, respectively.[19] The activating mutations in the G-protein-coupled receptor *CYSLTR2* or in the signal mediator *PLCB4* are detected in the remaining UM cases.[20,21] The constant activity of the Gα-protein signaling cascade leads to dysregulation of multiple downstream effectors such as protein kinase C (PKC), mitogen-activated protein (MAP) kinases, and yes-associated protein 1 (YAP) and causes uncontrolled proliferation of UM cells.[22,23] In addition to the somatic mutations in *GNAQ* and *GNA11*, UM is characterized by copy number variation of the chromosomes 1q, 3, 6p, and 8q.[24–27] Amplification of chromosome 8q and, especially, loss of chromosome 3 are strong prognostic factors for metastasis. Chromosome 3 carries the *BAP1* gene, encoding a ubiquitin hydrolase. *BAP1* is frequently found mutated in the remaining allele in UM with monosomy 3, which leads to complete loss of *BAP1* expression and strongly correlates with metastases development and poor prognosis.[28] Other factors of metastatic risk are the mutations in splicing modulators *SF3B1* and *SRSF2*.[19] The mutation in the translation initiation factor *EIF1AX*, in contrast, correlates with disomy of chromosome 3 and low risk of metastases.[29]

The absence of a targetable strong driver mutation may be one of the reasons why single-agent treatments have been ineffective for UM. The mutations in *GNAQ/11* lead to an imbalance in the wide signaling landscape instead of activating one specific pathway, and currently these mutant G-proteins cannot be selectively inhibited, although depsipeptides FR900359 and YM-254890 have shown promising results in preclinical experiments.[30] Therefore, combining several therapeutic agents targeting distinct signaling pathways might be beneficial, as it would allow suppressing multiple signaling cascades. In this work, we focused on examining the effect of dual combinations of several targeted compounds on the viability of UM cell lines, derived either from UM metastases or with the genetic background that corresponds to metastatic predisposition. We performed a small-scale drug screen of the four agents—trabectedin (Yondelis), foretinib, CX-4945 (silmitasertib), and RG7112—and their combinations on a panel of seven UM cell lines. (The characteristics of the compounds are summarized in Table 1, and the genetic aberrations of the UM cell lines are provided in Table 2.) These agents target the pathways reported to be important for the growth or metastatic spread of UM.[31–35] Our results show that the combinations of trabectedin with either CX-4942 or foretinib (at later stages replaced by cabozantinib) efficiently inhibit the growth of UM cells in cell culture and could be considered as putative therapeutics for metastatic UM.

Methods

Cell Culture and Lentiviral Transductions

Cell lines OMM2.5 (RRID:CVCL_C307), OMM2.3 (RRID:CVCL_C306), Mel285 (RRID:CVCL_C303), and Mel290 (RRID:CVCL_C304) (all a gift of Bruce Ksander), as well as OMM1 (RRID:CVCL_6939),[40] were cultured in a mixture of Roswell Park Memorial Institute (RPMI) 1640 Medium

(Thermo Fisher Scientific, Waltham, MA, USA) and Dulbecco's Modified Eagle Medium/Nutrient Mixture F-12 (DMEM-F12, 1:1; Thermo Fisher Scientific) supplemented with 10% fetal bovine serum (FBS) and antibiotics. MM28 (RRID:CVCL_4D15), MP38 (RRID:CVCL_4D11), MP46 (RRID:CVCL_4D13), and MM66 (RRID:CVCL_4D17)[41] were cultured in Iscove's Modified Dulbecco's Medium supplemented with 20% FBS and antibiotics. The cell lines were maintained in a humidified incubator at 37°C with 5% CO_2.

Inducible short hairpin RNA (shRNA) knockdown lentiviral vectors were constructed as described previously.[42,43] The production of lentivirus stocks by transfections into 293T (CVCL_0063) cells was carried out essentially as described previously, except that calcium phosphate was replaced with polyethylenimine.[44] Virus was quantitated by antigen capture enzyme-linked immunosorbent assay measuring human immunodeficiency virus p24 levels (ZeptoMetrix Corp., New York, NY, USA). Cells were transduced using a multiplicity of infection of 2 in medium containing 8 μg/mL polybrene. Target shRNA sequences to deplete Mer proto-oncogene tyrosine kinase (MERTK) or protein tyrosine kinase 3 (TYRO3) and the control sequences are shown in Supplementary Table S1.

Compound Screen

Cells were seeded in appropriate concentration in 6 × 6 wells in 96-well plates. The next day, the media were supplemented with serial dilutions of a single agent or a combination of two inhibitors. Six concentrations of each inhibitor were used. Viability was assayed after 5 days of treatment using the CellTiter-Blue Cell Viability Assay (Promega, Madison, WI, USA). In each experiment, technical triplicates were assessed, and all analyses were performed on three biological replicates. A putative synergistic effect was calculated using the excess over Bliss algorithm.[45,46] Foretinib, CX-4945, cabozantinib, INC280 (capmatinib), and RG7112 were obtained from Selleck Chemicals (Houston, TX, USA). Trabectedin was a gift from PharmaMar (Madrid, Spain).

Caspase 3 and 7 Activity

The cells were seeded in triplicate in white-walled 96-well plates with clear bottoms and in clear 96-well plates. The next day, the media were supplemented with the single agents or a combination of two inhibitors; the concentrations are listed in Supplementary Table S2. Five days later, caspase 3 and 7 activity was assessed with the use of the Caspase-Glo 3/7 Assay (Promega), and cell viability was assessed with the CellTiter-Blue Cell Viability Assay. The caspase activity relative to viability was then calculated.

Western Blot

The cells were seeded into six-well plates. The next day, the media were supplemented with a single drug or a combination of two agents; the concentrations are listed in Supplementary Table S3. After the treatments, the cells were rinsed twice with ice-cold PBS and scraped and lysed with Giordano Buffer (50-mM Tris-HCl, pH 7.4; 250-mM NaCl; 0.1% Triton X-100; 5-mM EDTA), supplemented with phosphatase- and protease inhibitors. Equal protein amounts were separated by sodium dodecyl sulfate–polyacrylamide gel electrophoresis and blotted on polyvinylidene fluoride membranes (MilliporeSigma, Darmstadt, Germany). The membranes were blocked with 10% non-fat dry milk in Tris-buffered saline with 0.1% Tween 20 Detergent (TBST; 10-mM Tris-HCl, pH 8.0; 150-mM NaCl; 0.2% Tween 20) and incubated with the primary antibody diluted in 5% BSA/TBST overnight at 4°C. The membranes were washed with TBST and incubated with horseradish peroxidase–conjugated secondary antibodies (The Jackson Laboratory, Bar Harbor, ME, USA). The chemiluminescent signal was visualized using X-ray film or a ChemiDoc Imaging System (Bio-Rad, Hercules, CA, USA). The analysis of the blots was performed using Image Lab software (Bio-Rad). The primary antibodies are listed in Supplementary Table S4.

Flow Cytometry

The cells were seeded into six-well plates. The next day, the media were supplemented with a single drug or a combination of agents; the applied concentrations are listed in Supplementary Table S5. After 5 days, the cells (including floating cells) were collected with trypsinization, washed two times with ice-cold PBS, and fixed with 70% ethanol overnight at 4°C. The cells were then washed with PBS containing 2% FBS; suspended in PBS containing 2% FBS, 50-µg/mL propidium iodide, and 50-µg/mL RNAse A; and incubated 30 minutes at 37°C. Flow cytometry was performed using the BD LSR II Flow Cytometer (BD Biosciences, Franklin Lakes, NJ, USA). In total, 10,000 events were recorded. The data were analyzed using FlowJo 10.6.1 software. The sum of the percentages of cells in G1, S, and G2 phases was set to 100. The subG1 population was determined as a percentage of the whole population.

RNA Isolation and Quantitative PCR

The cells were seeded into six-well plates. The next day, the media were supplemented with a single drug or a combination of agents; the concentrations are listed in Supplementary Table S2. After the treatment, the cells were collected by scraping in lysis buffer and RNA was isolated using the SV Total RNA Isolation System (Promega) according to the manufacturer's protocol. The reverse transcription reaction was performed using ImProm-II Reverse Transcriptase (Promega). Quantitative PCR was performed using SYBR Green (Roche, Basel, Switzerland) in a C1000 Touch thermal cycler (Bio-Rad). Relative expression of the tested genes was calculated compared to expression of housekeeping calcium-activated neutral proteinase 1 (CAPNS1) and signal recognition particle receptor (SRPR). The primer sequences are listed in Supplementary Table S6. Analysis of the effects of CX-4945 on mRNA splicing was performed with the primers listed in Supplementary Table S7.

In Vivo Experiments

UM Patient-Derived Xenograft Models. Three UM patient-derived xenograft (PDX) models (MM26, MM309, and MM339) obtained from human liver-metastatic UM were used. MM26 is mutated for *GNAQ* and *SF3B1*. MM309 is mutated for *GNAQ* and MM339 is mutated for *GNA11*, and both are mutated for *BAP1*.

Reagents. Trabectedin was kindly provided by PharmaMar and administered intravenously weekly. Cabozantinib and CX-4945 were purchased from MedchemExpress (Princeton, NJ, USA). Cabozantinib was formulated in a

vehicle of 3% dimethyl sulfoxide (DMSO), 30% polyethylene glycol 300 (PEG300), and 67% hydroxypropyl-β-cyclodextrin (HPCD; 20%). CX-4945 was formulated in 10% DMSO, 40% PEG300, 30% polypropylene glycol, and 20% H_2O. Cabozantinib was administered at 20 and 30 mg/kg daily and CX-4945 at 75 mg/kg twice daily. Both were administered orally 5 days per week.

In Vivo Efficacy Studies. For efficacy assessments, tumor fragments were transplanted into female severe combined immunodeficiency (SCID) mice from Janvier Labs (Le Genest-Saint-Isle, France). Xenografts were randomly assigned to the different treatment groups when tumors reached a volume of between 60 and 260 mm3. Tumor size was measured with a manual caliper twice per week. Tumor volumes were calculated as $V = a \times b^2/2$, where *a* is the largest diameter and b is the smallest. Tumor volumes were then reported compared to the initial volume as relative tumor volume (RTV). Means and SEMs of RTV in the same treatment group were calculated, and growth curves were established as a function of time. Antitumor activity was evaluated by determining tumor growth inhibition (TGI) as follows: percent GI = 100 − (RTVt/RTVc × 100), where RTVt is the mean RTV of treated mice and RTVc is the mean RTV of controls, both for the time point at which the antitumor effect was optimal. A meaningful biological effect was defined as TGI of at least 50%. The statistical significance of the differences observed between the individual RTVs corresponding to the treated and control mice was determined by two-tailed Mann–Whitney tests. Moreover, the responses to treatments in all models were evaluated as a function of individual mouse variability by considering each mouse as a single tumor-bearing entity. Hence, in all in vivo experiments, a relative tumor volume variation (RTVV) was calculated for each treated mouse as follows: (RTVt/mRTVc), where RTVt is the relative tumor volume of the treated mouse and mRTVc is the median relative tumor volume of the corresponding control group of corresponding day of treatment. We then calculated (RTVV)-1 for each treated mouse. A tumor was considered to be responding to treatment if (RTVV)-1 was below −0.5. Finally, to assess the impact of treatments on the tumor progression, we evaluated the probability of progression (doubling time) as described previously.[47]

This study was performed in accordance with the recommendations of the European Community (2010/63/UE) for the care and use of laboratory animals. Experimental procedures were approved by the ethics committee of Institut Curie CEEA-IC #118 (Authorization APAFIS# 25870-2020060410487032-v1 given by National Authority) in compliance with international guidelines.

Clinical Data Analysis

The Leiden University Medical Centre (LUMC) cohort includes clinical, histopathological, and genetic information on 64 UM cases enucleated between 1999 and 2008 at the LUMC. Clinical information was collected from the Integral Cancer Center West patient records and updated in 2021. For each sample, part of the tumor was snap frozen with 2-methylbutane and used for mRNA and DNA isolation; the remainder was embedded in paraffin after 48 hours of fixation in 4% neutral-buffered formalin and was sent for histological analysis. RNA was isolated with the RNeasy Mini Kit (QIAGEN, Hilden, Germany), and mRNA expression was determined with the HT-12 v4 BeadChip (Illumina, San Diego, CA, USA). BRCA1-associated protein 1 (BAP1) status (positive or negative) was determined by immunohistochemistry. The Cancer Genome Atlas (TCGA) cohort represents 80 primary UM cases enucleated in six different centers.[48] mRNA expression was determined by RNA sequencing. BAP1 status (high or low expression) was determined by splitting mRNA expression along the median expression value.

Statistical analyses of the LUMC and TCGA cohorts were carried out using SPSS Statistics 25 (IBM Corp., Chicago, IL, USA). For survival analysis, Kaplan–Meier and log-rank tests were performed, with death due to metastases as the endpoint. Cases that died of another or unknown cause were censored. The two subpopulations that were compared in each analysis were determined by splitting the total cohort along the median value of mRNA expression for each analyzed gene. The study was approved by the Biobank Committee of the LUMC (19.062.CBO/uveamalanoomlab-2019-3; B20.023). The tenets of the Declaration of Helsinki were followed.

Results

Identification of the Synergistic Combinations

We performed a screen of dual combinations of the inhibitors trabectedin, foretinib, CX-4945, and RG7112 (Table 1) on a panel of seven uveal melanoma cell lines derived either from UM metastases or from primary tumors not expressing BAP1, a strong factor for poor prognosis (Table 2). We assessed the effect of the drug combinations on cell viability after 5 days of the treatment; based on the effect matrix, we calculated the synergistic score of the combinations using the excess over Bliss algorithm[45] (Supplementary Fig. S1A). Figure 1A represents the matrix of the highest calculated excess over Bliss score of each treatment per cell line. The combinations of RG7112 either demonstrated low excess over Bliss values (RG7112 with foretinib) or were synergistic only in a subset of the cell lines (RG7112 with trabectedin or CX-4945), whereas the combination of CX-4945 with foretinib or the combination of trabectedin with either CX4945 or foretinib showed positive synergistic scores across most of the tested cell lines. Figures 1B and 1C and Supplementary Figures S1B to S1E illustrate the effect of trabectedin combined with either CX-4945 or foretinib on survival of UM cell lines. It is worth noting that all of the tested UM cell lines are sensitive to trabectedin in picomolar concentrations. The combinations of trabectedin with either CX-4945 or foretinib reduced the survival of the cells more effectively than either of the single treatments, and fewer than 10% of the cells were viable at the highest tested concentrations after 5 days of treatment. Taking into account the significant effect of the combinations on cell survival and the high synergy scores, we chose the combination of CX-4945 with foretinib or the combination of trabectedin with either CX-4945 or foretinib for further investigation.

Combination of Trabectedin With Either CX-4945 or Foretinib Stimulates Apoptosis in UM Cell Lines

Next, we decided to examine the mechanism of action of the selected drug combinations. We assayed the activity of caspases 3 and 7 to clarify whether the selected combinations induce apoptosis (Figs. 1D–1F). Caspase 3 and 7

Investigative Ophthalmology & Visual Science

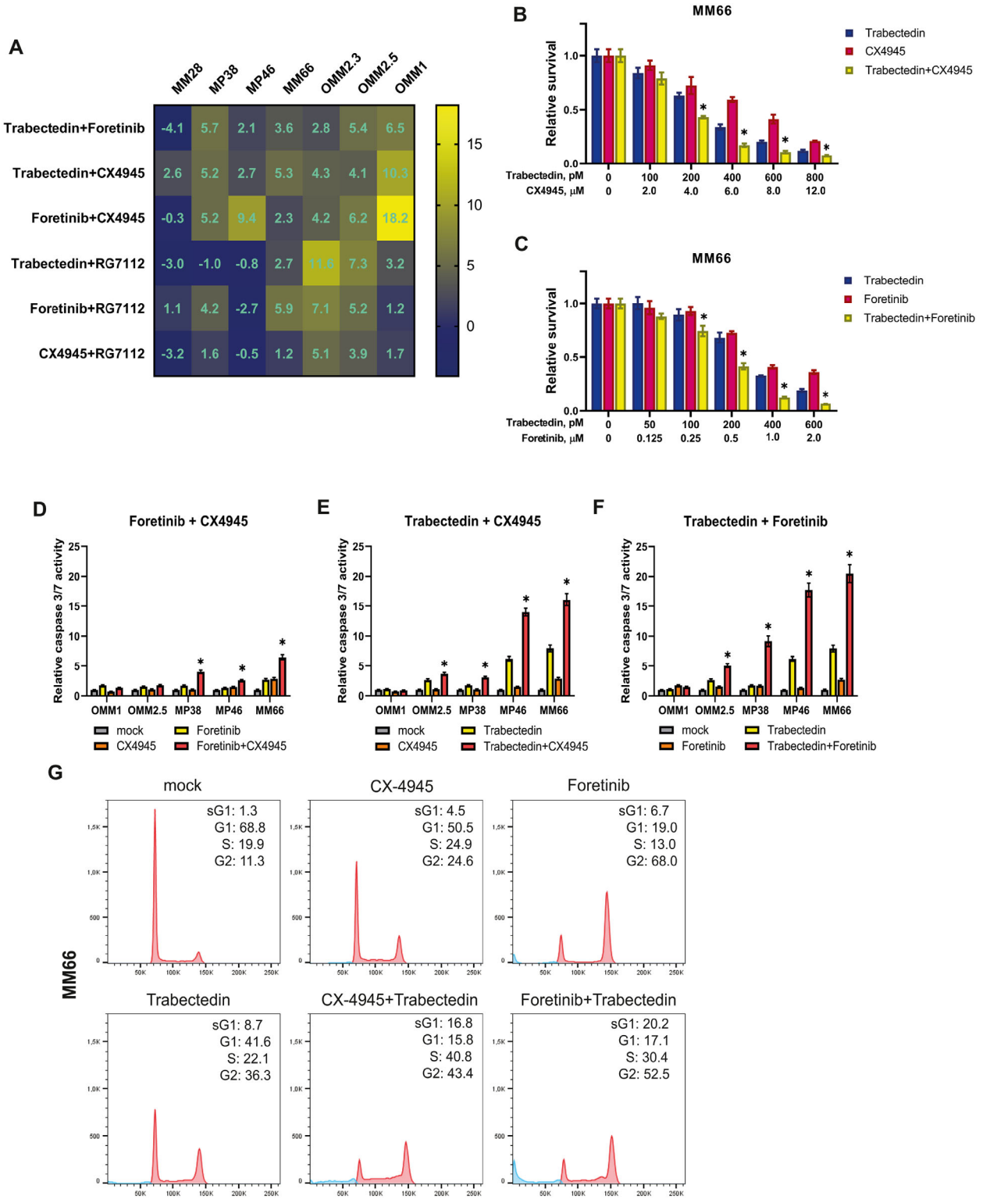

Figure 1. Trabectedin synergizes with CX-4945 and with foretinib in growth inhibition and apoptosis induction in UM cell lines. (**A**) The matrix of the highest excess over Bliss (EoB) synergy scores of each treatment per cell line. (**B**, **C**) Effect of trabectedin (*blue bars*), CX-4945 (**B**), or foretinib (**C**) (*magenta*) and their combination (*yellow*) on MM66 cell viability after 5 days of treatment. Significant ($P < 0.05$) reduction of viability in the combined treatment compared to both of the single treatments is indicated with an asterisk (*). Statistical analysis was performed using one-way ANOVA. *Error bars* indicate mean ± SEM ($n = 3$). (**D–F**) Induction of apoptosis in UM cell lines by the most synergistic combinations. Activity of caspases 3 and 7 was measured after 5 days of treatment; significant ($P < 0.05$) elevation of caspase 3 and 7 activity in the combined treatment compared to both of the single treatments is indicated with an asterisk (*). Statistical analysis was performed using one-way ANOVA. *Error bars* indicate mean ± SEM ($n = 3$). The concentrations of the compounds are listed in Supplementary Table S2. (**G**) Effect of trabectedin alone or in combination with either CX-4945 or foretinib on cell cycle progression of MM66 after 3 days of treatment. At least three independent replicates were performed, and a representative experiment is shown. The concentrations of the compounds are listed in Supplementary Table S5.

Investigative Ophthalmology & Visual Science

activity rose less than twofold for treatment with either CX-4945 or foretinib, whereas it showed variable increases from 1.1-fold in OMM1 to 7.9-fold in MM66 upon trabectedin treatment. In general, the effect of the combination of CX-4945 and foretinib was less pronounced than the effect of the combinations of trabectedin with either CX-4945 or foretinib. The combination of CX-4945 and foretinib (Fig. 1D) increased caspase activity in MP38 (fourfold), MP46 (2.6-fold), and MM66 (6.5-fold). The combination of trabectedin with either CX-4945 (Fig. 1E) or foretinib (Fig. 1F) strongly activated caspases 3 and 7 in most of the tested cell lines. The highest effect was observed in the combination of trabectedin and foretinib, as the relative caspase 3 and 7 activity increased five times in OMM2.5, 9.2 times in MP38, and 17.8 and 20.5 times in MP46 and MM66, respectively. The effect of the single or any combined treatment on the line OMM1 was minor; the relative caspase activity did not reach a twofold increase in any case. Because the combinations containing trabectedin demonstrated more potent activation of caspases 3 and 7 than the combination of CX-4945 and foretinib, we narrowed our further study to these two combinations.

In order to clarify the mechanism of action of the selected combinations in more detail, we examined their effect on cell cycle progression for the following UM cell lines: MM66, MP38, MP46, OMM1, and OMM2.5 (Fig. 1G, Supplementary Figs. S1F–S1I). The cells treated with foretinib alone were arrested in the G2 phase. Monotreatment with CX-4945 also led to the accumulation of cells in the G2 phase, but to a lesser extent than did foretinib. The cells treated with trabectedin alone accumulated in the S and G2 phases. The number of subG1 cells, indicating cell death, increased significantly upon treatment with trabectedin but less so with CX-4945 or foretinib treatment. These effects were substantial in MM66, MP38, and MP46 but less pronounced in OMM1 and OMM2.5.

The cells treated with the combination of trabectedin with either CX-4945 or foretinib were arrested in the G2 phase. The number of the cells in the subG1 fraction rose drastically compared to single treatment in the cell lines MM66, MP46, and MP38, but the effect on OMM1 was less pronounced, which correlated with the aforementioned induction of caspase 3 and 7 activity. The significant increase in subG1 cells confirms the synergism of the combinations and the induction of cell death due to the treatments.

The induction of apoptosis is regulated by several factors, including the balance in expression of Bcl2 family members; therefore, we evaluated the expression of several of these genes after 24 hours of treatment. In general, expression of the anti-apoptotic gene *Bcl-2* decreased, and expression of the pro-apoptotic genes *Bim* and *Bmf* increased after treatment with the combination of CX-4945 and trabectedin (Fig. 2A). The effect of the combination of trabectedin and foretinib on the expression of the tested genes was less explicit, and it varied per cell line (Fig. 2B). Expression of other Bcl2 family members either was not affected or occurred only in a subset of the tested cell lines.

Verification of the Target Engagement of the Selected Compounds

CX-4945 Targets Casein Kinase 2 and Affects Splicing. To verify the target engagement of the selected compounds, we performed immunoblots and mRNA analyses in a subset of the cell lines representing both GNA11 and GNAQ mutations and BAP1-positive or -negative status. The concentrations of the compounds corresponded to 50% growth inhibition after 5 days. The treatment with CX-4945 reduced the phosphorylation of AKT at serine 129, the reported casein kinase 2 phosphorylation site (Fig. 2C).[49] Additionally, CX-4945 has been shown to affect Cdc2-like kinases (CLKs), which are essential for the regulatory phosphorylation of SRSF proteins involved in splicing control.[50] To examine this effect in UM, we analyzed the splicing of *Ell* mRNA and *Mdmx* mRNA.[51] Effects on *Ell* splicing were found in three tested cell lines, the most pronounced being in MM66 cells after 8 hours of treatment (Fig. 2D). Moreover, CX-4945 changed the balance between *Mdmx-FL* and *Mdmx-S* mRNA; again, the effect was strongest in MM66 cells and after 8 hours of treatment.

Trabectedin Induces DNA Damage Response. Trabectedin interacts with the "minor groove" of DNA, activating a DNA damage response cascade, among its many biological effects. The downstream targets of trabectedin were examined in the experiments investigating the trabectedin combinations in four cell lines (MP38, MP46, MM66, and OMM1) treated for 24 hours. The results of protein analyses upon treatment with trabectedin, CX-4945, or their combination are presented in Figure 2E and Supplementary Figure S2A. The treatment with trabectedin resulted in phosphorylation and stabilization of p53 as a consequence of the DNA damage, in agreement with previous reports.[52,53] Increased *Mdm2* and *CDKN1A* mRNA levels could be observed, indicating activation of p53 transcriptional activity (Supplementary Fig. S2B).

Foretinib Inhibits Activity of c-MET and TAM Receptors. Foretinib has been reported to inhibit activity of c-MET, vascular endothelial growth factor receptor 2 (VEGFR2), and the TAM receptors (TYRO3, Axl, MERTK). Activated c-MET, as determined by phosphorylation on tyrosines 1234/1235, is not or barely detectable in most UM cell lines, with medium detection in MP46 and MP38 and being just detectable in OMM1, OMM2.3, OMM2.5, and MM28 cells (see Supplementary Fig. S2C). Expression of Axl could not be detected in any metastatic UM cell line or a primary *BAP1*-negative cell line, although Axl is expressed in Mel285 and Mel290, which are primary UM cell lines not carrying *GNAQ/11* mutations. In contrast, MERTK is highly expressed in the tested cell lines, except for Mel285 and Mel290. TYRO3 is abundantly present in all of the tested UM cell lines, which is in agreement with the observation that the expression of TYRO3 is highest in uveal melanoma among all tumor types analyzed in the cBioportal.org database.[54,55] Inhibition of the receptor tyrosine kinases by foretinib (alone or in combination with trabectedin) resulted in moderation of AKT signaling, which is illustrated in Figure 2F and Supplementary Figure S2D, by depletion of phosphorylation of AKT at serine 473 and a drop in phosphorylation of its downstream target proline-rich AKT substrate of 40 kDa (PRAS40).

To show the effect of foretinib on activated c-MET, we incubated MP46 cells (not pretreated or pretreated with either foretinib or cabozantinib, another clinically relevant c-MET inhibitor) with a mixture of growth arrest-specific 6 (GAS6; the ligand of TAM receptors) and hepatocyte growth factor (HGF; the ligand of c-MET), which stimulated both c-MET phosphorylation and activation of the TAM receptors. Both foretinib and cabozantinib strongly diminished the level of phosphorylated c-MET and reduced the amount of activated AKT and extracellular-regulated kinase (ERK), indicating the efficacy of these compounds (Fig. 2G).

Investigative Ophthalmology & Visual Science

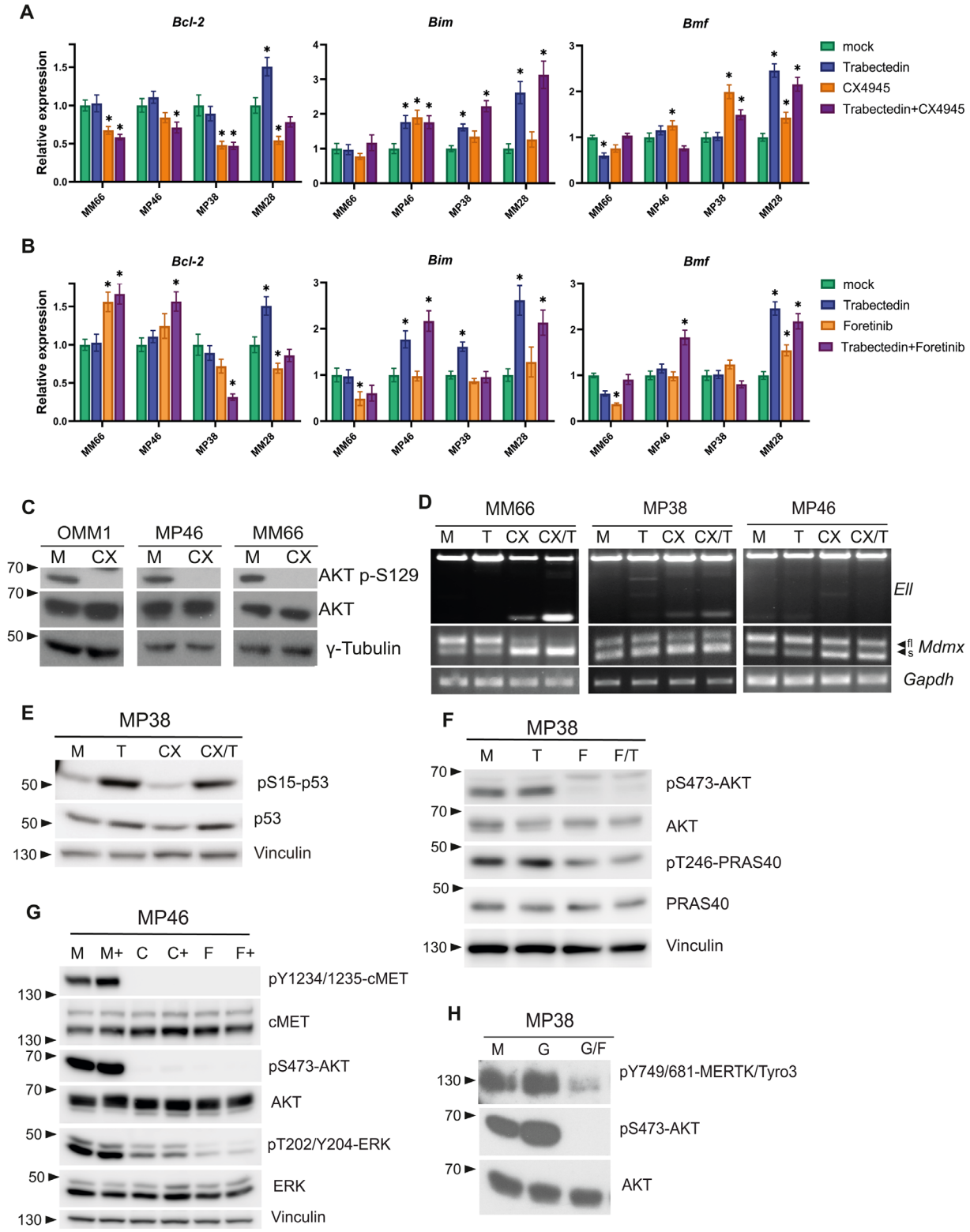

Figure 2. Molecular effects of trabectedin, CX-4945, and foretinib. (**A**, **B**) Expression of *Bcl-2*, *Bim*, and *Bmf* mRNA upon 24-hour treatment with trabectedin in combination with CX-4945 (**A**) or foretinib (**B**) in UM cell lines. Significant ($P < 0.05$) change in mRNA expression compared to the control is indicated with an asterisk (*). Statistical analysis was performed using one-way ANOVA. *Error bars* indicate mean ± SEM ($n = 3$). The concentrations of the compounds for this and the following experiments are listed in Supplementary Table S3, if not specified. (**C**) The effect of treatment with CX-4945 (CX) for 24 hours on phosphorylation of AKT on S129, a reported casein kinase 2 phosphorylation site. γ-Tubulin expression was used as a loading control. (**D**) The effect of treatment with trabectedin (T), CX-4945 (CX), or their combination (CX/T) for 8 hours on splicing of the *Ell* and *Mdmx* mRNA. *Gapdh* mRNA expression was used as a control. (**E**, **F**) MP38 cells either were not treated (M) or were treated with trabectedin (T), CX-4945 (CX), or the combination (CX/T) (**E**) or foretinib (**F**) or the combination (F/T) (F) for 24 hours, after which cells were harvested and the expression of the indicated proteins was analyzed. Vinculin was used as a loading control. (**G**) MP46 cells were grown on 0.5% fetal bovine serum (FBS) for 6 hours. Subsequently, they either were not pretreated (M) or were pretreated with either foretinib (F; 4 µM) or cabozantinib (C; 4 µM) for 2 hours, after which the cells were either not

stimulated or stimulated with a mixture of HGF and GAS6 (50 and 300 ng/mL, respectively, indicated with +) for 20 minutes, then the cells were harvested for protein lysates. (**H**) MP38 cells grown in 0.5% serum for 6 hours either were not pretreated (M) or were pretreated with foretinib (F; 4 µM) for 2 hours, after which both untreated and foretinib pretreated cells were then stimulated with GAS6 (G; 300 ng/mL) for 20 minutes and collected for analysis. Total AKT was used as a loading control.

Additionally, we compared the effect of foretinib and the specific c-MET inhibitor INC280 (capmatinib) on UM cells stimulated with HGF. MP38 cells, serum-starved overnight, were pre-incubated with vehicle, foretinib, or INC280 for 2 hours. Subsequently, the cells were treated with either vehicle or HGF for 20 minutes. The treatment with HGF strongly increased the levels of activated c-MET, activated AKT, and activated ERK (Supplementary Fig. S2E). Both foretinib and INC280 completely abrogated the stimulation of c-MET; however, INC280 only prevented the HGF effect, but foretinib reduced the levels of activated AKT and ERK beyond basal, low serum levels, suggesting the inhibition of additional targets apart from c-MET. Moreover, foretinib and cabozantinib had an effect on UM cell growth, but INC280 did not inhibit proliferation of all the tested cell lines, irrespective of their basal c-MET activity (Supplementary Fig. S2F). Therefore, specific inhibition of c-MET might not be sufficient for blocking the growth of UM metastases.

To investigate the impact of foretinib on the activity of TAM receptors in UM cells, we pretreated MP38 (grown in 0.5% serum for 6 hours) with foretinib or vehicle for 2 hours, then stimulated the cells with GAS6, an activating ligand for TAM receptors. The results presented in Figure 2H demonstrate that GAS6 stimulation increased the levels of activated AKT, an effect that was completely abrogated by foretinib treatment, thus indicating the efficacy of foretinib against the TAM receptors. The phosphorylation of TYRO3/MERTK was increased by GAS6 and was strongly reduced by foretinib treatment.

Inhibition of MERTK Is Important for Synergistic Combination With Trabectedin. In order to clarify the importance of inhibiting TAM receptors combined with trabectedin treatment, we generated derivatives from the UM cell line OMM2.5 containing vectors for doxycycline-inducible knockdown of either *TYRO3* (Fig. 3A) or *MERTK* (Fig. 3B). The protein levels of MERTK and TYRO3 dropped significantly upon induction of corresponding shRNAs. Moreover, we noticed that the level of MERTK decreased upon induction of shTYRO3 #2 and #3, as well.

The depletion of expression of both proteins led to retardation of cell growth; however, the effect of MERTK knockdown was greater than the depletion of TYRO3. After 4 days of doxycycline induction, expression i-shTYRO3 #2 slowed down the growth of OMM2.5 cells, whereas the effect of the other i-shTYRO3 appeared only after 6 days of induction (Fig. 3C). Growth retardation of the cells expressing shMERTK was apparent already after 4 days of induction, and only about 25% of the cells were left viable 2 days later (Fig. 3D).

When the knockdown of MERTK was combined with various doses of trabectedin, we detected additional growth reduction, and the positive values of excess over Bliss scores indicated synergism (Fig. 3F). The effect of trabectedin alone on survival was even stronger than that of the combinations with shTYRO3 #1, indicating an action that was not additive and perhaps even slightly antagonistic. However, synergism was observed in the case of i-shTYRO3 #2 (Fig. 3E). This effect could be due to the simultaneous decline of the expression of both TYRO3 and MERTK by shTYRO3 #2. Downregulation of MERTK by this shRNA was most likely indirect, because it took place only after the prolonged treatment with doxycycline, and the sequences targeting *TYRO3* mRNA are very different from the sequences in *MERTK* mRNA.

The synergistic effect of the combination of MERTK knockdown and trabectedin was also demonstrated by the analysis of cleaved poly(ADP-ribose)polymerase (PARP), a marker of apoptosis (Fig. 3B). The level of cleaved PARP was elevated (and the level of full-length PARP dropped) after treatment with the combination of doxycycline and trabectedin compared to the single treatments; the effect was also valid for shTYRO3 #2 but was less pronounced in shTYRO3 #1 and #3 (Fig. 3A).

Confirming the results upon depletion of MERTK, we found that UM cell lines are sensitive in a low micromolar range to pharmacological inhibition of MERTK by UNC569, as illustrated in Figure 4A and Supplementary Figure S3A. The combination of UNC569 with trabectedin synergistically slowed down the growth of UM cell lines, resembling the effects of trabectedin in MERTK-depleted cells. The target engagement of UNC569 is demonstrated in Figure 4B. UM cell lines OMM1, MM66, and MP46 either not pretreated or pretreated with UNC569 were stimulated with the ligand of TAM receptor GAS6. The addition of GAS6 activated AKT signaling, thus increasing the phosphorylation of AKT at Ser473, but pretreatment with UNC569 completely blocked this upregulation. Overall, these results indicate the importance of inhibition of TAM receptors, especially MERTK, with regard to the growth of UM cell lines and the synergistic effect of the combination with trabectedin.

Having demonstrated the effect of MERTK control on the proliferation of UM cells, we decided to examine if expression of MERTK or its ligands could be related to the metastatic potential of UM and survival of patients with metastatic UM. We analyzed mRNA expression of *MERTK*, *GAS6*, and *PROS1* in two cohorts of patients with UM. The LUMC cohort included 64 cases (Figs. 4C, 4F; Supplementary Fig. S3F), and the TCGA cohort included 80 cases (Supplementary Figs. S3B, S3C, S3H). We stratified the cases by the expression of BAP1, as the loss of BAP1 expression represents a crucial predisposing factor for the development of UM metastases. The mRNA expression of *GAS6* turned out to be significantly elevated in BAP1-negative tumors compared to BAP1-positive tumors in both cohorts (Fig. 4C, Supplementary Fig. S3B). A similar increase of *PROS1* expression was found only in the TCGA cohort (Supplementary Fig. S3C) but not in the LUMC cohort (Fig. 4F). The mRNA expression of *MERTK* did not differ between the BAP1-positive and BAP1-negative groups in either cohort (Supplementary Figs. S3F, S3H).

The mRNA expression of *GAS6* and *PROS1* was negatively correlated with survival of patients with UM in the LUMC cohort, as demonstrated in Figures 4D and 4F. However, in the TCGA cohort, we found a significant effect of *PROS1* expression on survival (Supplementary Fig. S4E), but not *GAS6* expression (Supplementary Fig. S3D). The mRNA

Investigative Ophthalmology & Visual Science

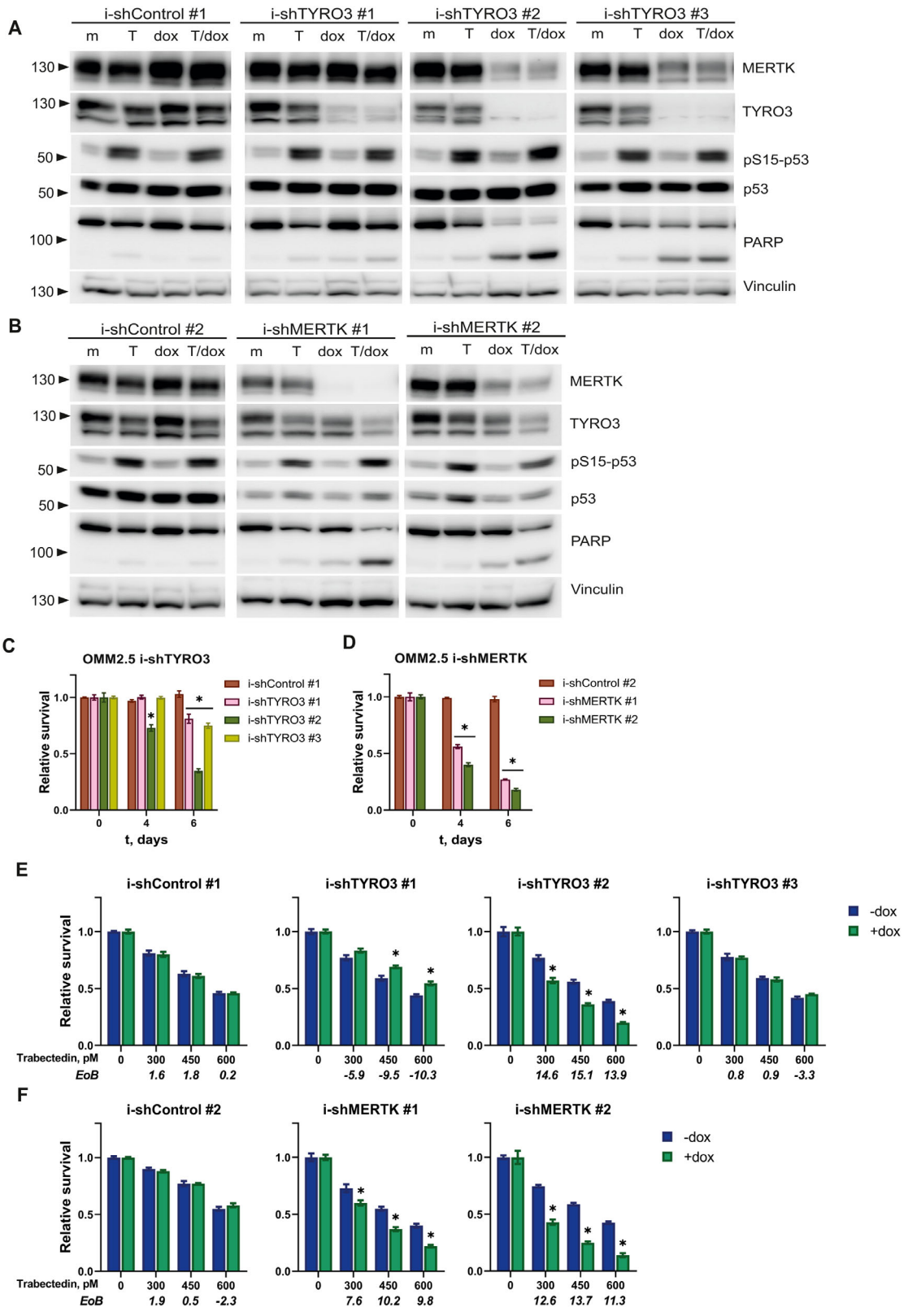

Figure 3. Effects of genetic depletion of TYRO3 and MERTK in combination with trabectedin on UM cells. (**A**, **B**) OMM2.5 cells containing i-shControl or i-shTYRO3 vectors (**A**) or i-shMERTK vectors (**B**) were seeded into six-well plates. Next day, the cells were treated with either 30 ng/mL doxycycline (dox) or vehicle (m). Two days later, all wells were refreshed with medium with or without doxycycline and with or without 300 pM trabectedin (T). This treatment was repeated every other day for a total duration of 7 days of doxycycline (5 days of trabectedin). (**C**, **D**) OMM2.5 cells containing i-shControl or i-shTYRO3 vectors (**C**) or i-shMERTK vectors (**D**) were seeded into duplicate 96-well plates; at the end of the same day, when the cells were attached, the medium was supplemented with 30 ng/mL doxycycline (20 ng/mL in the case of i-shTYRO3 #2). Medium plus or minus doxycycline was refreshed every other day. The plates were analyzed after 4 days and duplicate plates after 6 days. Significant reduction ($P < 0.05$) of viability compared to control (day 0) is indicated with an asterisk (*). Statistical analysis was performed using one-way ANOVA. *Error bars* indicate mean ± SEM ($n = 3$). (**E**, **F**) OMM2.5 cells containing either

i-shControl or i-shTYRO3 vectors (**E**) or i-shMERTK vectors (**F**) were seeded into 96-well plates; at the end of the same day, when cells were attached, the medium in half of the wells was supplemented with 30 ng/mL doxycycline (20 ng/mL in the case of i-shTYRO3 #2). The next day (day 1), trabectedin was added; at day 2 the treatment with doxycycline and trabectedin was refreshed, and at day 4 cell viability was assessed. Significant ($P < 0.05$) difference in viability of doxycycline-treated samples compared to vehicle-treated samples is indicated with an asterisk (*). Statistical analysis was performed using *t*-test. *Error bars* indicate mean ± SEM ($n = 3$).

expression of *MERTK* did not affect UM-related death in any of the cohorts (Supplementary Figs. S3G, S3I). The correlation of the expression of the ligands *GAS6* and *PROS1* with BAP1 status and survival of patients with UM highlights the significance of MERTK activity for metastases progression in such patients.

Cabozantinib Mimics the Synergistic Effects of Foretinib in Combination With Trabectedin

The main purpose of our project was to investigate potential therapeutic options for the patients with metastatic UM. Because the commercial development of foretinib was discontinued during the course of our studies, we decided to substitute cabozantinib for foretinib for the experiments in vivo. Cabozantinib has been approved by the U.S. Food and Drug Administration (FDA) for metastatic differentiated thyroid cancer and is currently undergoing clinical studies for advanced tumors of other types,[56] including uveal melanoma.[57]

We were able to reproduce the results of the in vitro experiments when foretinib was replaced by cabozantinib. The UM cell lines were sensitive to cabozantinib in micromolar concentrations (Supplementary Fig. S2F), and the effect on survival was synergistically enhanced in combination with trabectedin (Fig. 5A, Supplementary Fig. S3A). The combination of trabectedin and cabozantinib strongly induced caspase 3 and 7 activity in the tested UM cell lines, as demonstrated in Figure 5B. Cabozantinib, as well as foretinib, efficiently inhibited the signaling of both c-MET and TAM receptors, which is demonstrated in Figure 2G. The results of the combinations of trabectedin and cabozantinib with CX-4945 were promising in cell culture experiments. Therefore, it was decided to test the efficacy of these combinations on UM PDX models in vivo.

In Vivo Experiments

Three different UM PDXs were included in our in vivo experiments: MM26, MM309, and MM339. The change in RTV for each treatment is shown in Figure 5C. The overall response rate (ORR) is shown in Supplementary Figure S4B, and Figures 5D and 5E show the cumulative probability of tumor progression (doubling time) for all three models. Looking at the efficacy of each tested monotherapy, we observed that trabectedin alone induced TGIs of 42% ($P = 0.0157$), 49%, and 35% in MM26, MM309, and MM339 PDXs, respectively (ORR = 47%). CX-4945 demonstrated a slight antitumor activity in MM26 and MM339 models; the effect was more profound on the MM309 PDX (ORR = 27%). Inversely, cabozantinib blocked tumor growth in all treated PDXs in both tested dosages (ORR = 100% in the 20-mg/kg/day group; ORR = 93% in the 30-mg/kg/day group). We did not observe additive efficacy after combining trabectedin with CX-4945 administration. Similarly, we did not observe an additive effect after the administration of trabectedin in combination with cabozantinib, regardless of cabozantinib dosage.

Discussion

In recent years, various therapeutics have been developed and tested in clinics in order to improve outcomes for patients with metastatic UM.[8] DNA-damaging chemotherapeutics, mainly alkylating agents, have been widely investigated as potential therapy for metastatic UM, but so far they have demonstrated limited effect on overall survival.[58–61] Trabectedin is a DNA-damaging agent with a distinct, complex mechanism of action. It binds to DNA minor grooves, forms adducts, and bends DNA, causing a DNA damage response. It also interacts with proteins bound to DNA, such as Rad13, and affects DNA repair and transcription.[62] In addition, trabectedin affects the tumor microenvironment and activates an immune response.[63] Trabectedin has been approved by the FDA as a second-line therapy for metastatic soft tissue sarcoma and has been tested clinically for the treatment of various types of solid tumors.[64,65]

In this study, we have shown that trabectedin inhibits proliferation and induces apoptosis in UM cell lines, and combining trabectedin with the CK2/CLK inhibitor CX-4945 reduces survival even further. CK2 phosphorylates a wide set of substrates, and inhibition of this kinase leads to alterations in multiple metabolic pathways.[66,67] Because trabectedin has multiple targets, it is not possible to pinpoint the key targets underlying the synergistic effect of these compounds. CX-4945 has previously been shown to enhance the effect of other DNA-targeting chemotherapeutics (e.g., cisplatin, carboplatin, gemcitabine, temozolomide, doxorubicin)[68] in the context of various solid tumors and hematological cancers. These promising preclinical results have instigated a clinical trial for treatment of cholangiocarcinoma by combining CX-4945 with cisplatin and gemcitabine.[68] Also, CX-4945 inhibits the activity of the cdc2-like kinases, which are indirectly involved in splicing; however, the importance of the latter function of CX-4945 for its anti-proliferative effect is unknown. We found that CX-4945 affects splicing of *Mdmx* mRNA, and targeting MDMX has been previously suggested as a therapeutic option for cells expressing wild-type p53.[51] The splicing machinery is often affected in UM, as 15% of the tumors carry mutation in splicing factor SF3B1.[33,69]

Trabectedin significantly inhibited UM PDX tumor growth in mouse models; however, CX-4945 did not significantly affect tumor growth in vivo, and it did not enhance the effect of trabectedin. Multiple explanations are possible; for example, perhaps CX-4945 could not sufficiently penetrate the solid, subcutaneous tumors formed by the PDX models. In conclusion, combinatory treatment with trabectedin and CX-4945, which was promising in vitro, cannot be confirmed in the in vivo PDX models, thus it is not a promising treatment for patients with metastatic UM. The other combination we investigated was trabectedin with foretinib, a c-MET and TAM receptor inhibitor. This combination also synergistically inhibited UM cell proliferation and

Investigative Ophthalmology & Visual Science

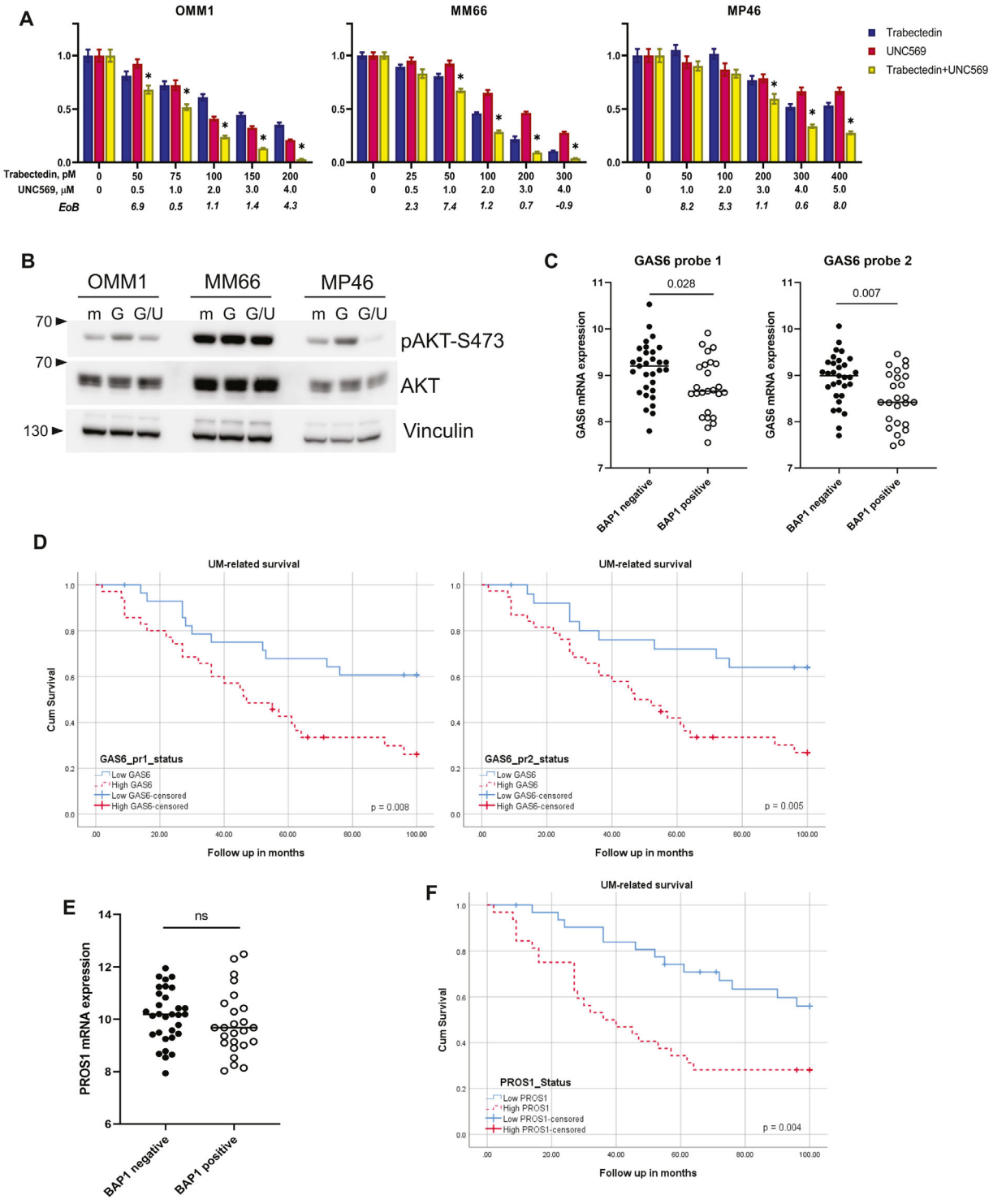

Figure 4. The higher mRNA expression of TAM receptor ligands *GAS6* and *PROS1* correlates with BAP1-negative status of the tumors and worse prognosis for patients with UM. (**A**) The effect of trabectedin (*blue bars*), UNC569 (*magenta*), and their combination (*yellow*) on the viability of OMM1, MM66, and MP46 cells after 5 days of treatment. Significant ($P < 0.05$) reduction of viability in combined treatment compared to both of the single treatments is indicated with an asterisk (*). Statistical analysis was performed using one-way ANOVA. *Error bars* indicate mean ± SEM ($n = 3$). (**B**) UM cell lines were seeded into six-well plates; the next day, the medium was supplemented with UNC569 (5 µM). Six hours later, 300 ng/mL GAS6 was added, and 20 minutes later the samples were harvested for analysis. m-control, G-GAS6-treated samples; G/U, UNC569- and GAS6-treated samples. (**C**) Correlation of *GAS6* mRNA expression with BAP1 status of the tumors in the LUMC cohort. The *left plot* represents probe 1; the *right plot*, probe 2. (**D**) Analysis of UM-specific survival related to *GAS6* expression in the LUMC patient cohort ($n = 64$). *GAS6* status is split at inflection point; the *left plot* represents probe 1 ($n = 29$ low, $n = 35$ high), and the *right plot* represents probe 2 ($n = 26$ low, $n = 38$ high). (**E**) Correlation of *PROS1* mRNA expression with the BAP1 status of tumors in the LUMC cohort. (**F**) Analysis of UM-specific survival related to *PROS1* expression in the LUMC patient cohort ($n = 64$; split at the median, $n = 32$ high and $n = 32$ low).

Investigative Ophthalmology & Visual Science

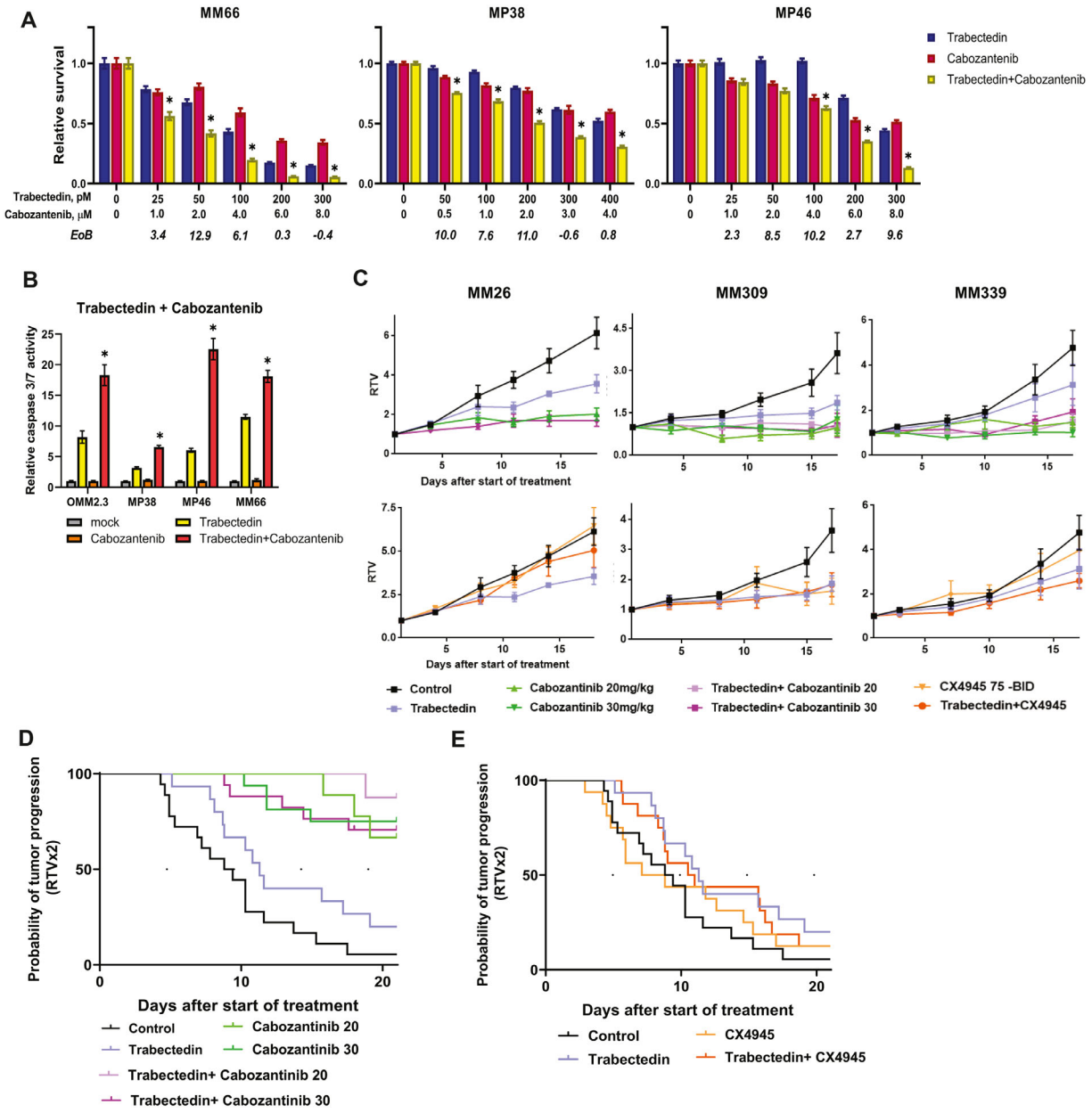

Figure 5. Cabozantinib, similar to foretinib, is synergistic with trabectedin in vitro, but not in vivo. (**A**) The effect of trabectedin (*blue bars*), cabozantinib (*magenta*), and their combination (*yellow*) on the viability of MM66, MP38, and MP46 cells after 5 days of treatment. Significant ($P < 0.05$) reduction of viability in combined treatment compared to both of the single treatments is indicated with an asterisk (*). Statistical analysis was performed using one-way ANOVA. *Error bars* indicate mean ± SEM ($n = 3$). (**B**) Induction of apoptosis in UM cell lines by trabectedin, cabozantinib, or the combination. The activity of caspases 3 and 7 was measured after 5 days of treatment; 200 pM of trabectedin was applied to MM66 and OMM2.3, 400 pM to MP38 and MP46, 4 μM of cabozantinib to MP38 and MM66, and 8 μM to OMM2.3 and MP46. Significant ($P < 0.05$) elevation of caspase 3 and 7 activity in combined treatment compared to both of the single treatments is indicated with an asterisk (*). Statistical analysis was performed using one-way ANOVA. *Error bars* indicate mean ± SEM ($n = 3$). (**C**) RTV upon treatment with trabectedin, cabozantinib, CX-4945, or combinations. The UM PDXs MM26, MM309, and MM339 were treated with trabectedin (0.125 mg/kg intravenously weekly), cabozantinib (20 or 30 mg/kg daily, 5 days per week), CX-4945 (75 mg/kg twice a day, 5 days per week), or a combination of the drugs. Tumor growth was evaluated by plotting mean RTV ± SEM for each group. For MM26, $n = 6$ independent PDX (trabectedin, trabectedin + CX-4945); $n = 7$ independent PDX (control, cabozantinib, CX-4945); and $n = 8$ (trabectedin + cabozantinib). For MM309, $n = 4$ for all groups except control and CX-4945 ($n = 5$). For MM339, $n = 5$ for all groups except control and trabectedin + cabozantinib (20 mg/kg, $n = 6$). (**D**, **E**) Probability of progression after trabectedin treatment with or without cabozantinib at 20 and 30 mg/kg daily (**D**) or CX-4945 at 75 mg/kg twice a day (**E**), taking tumor doubling time into account.

induced apoptosis. The c-MET inhibitors have been previously investigated as putative therapeutics for metastatic UM.[70] HGF, the ligand of c-MET, is abundantly present in the liver (the most common site of UM metastatic lesions) and stimulates activation of the receptor.[34,71] According to our data, specific inhibition of c-MET activity with the selective inhibitor INC280 does not affect UM cell proliferation in vitro, although it does not exclude an effect of c-MET

inhibition on the growth of UM metastases in patients. The treatment with foretinib inhibited the growth of UM cells, as it affects other targets besides c-MET (e.g., signal transduction of receptor tyrosine kinases MERTK and TYRO3) that are highly expressed in UM. Blocking of MERTK rather than TYRO3 activity synergizes with trabectedin, as follows from our experiments with genetic depletion of these receptors. Similarly, MERTK has been considered to be the main target of foretinib in glioblastoma, and the combination of foretinib with the DNA-damaging chemotherapeutic agent temozolomide has been reported to inhibit cell proliferation more efficiently than the single treatments.[72] It has been demonstrated that the level of MERTK increases after treatment with several alkylating agents,[73] indicating a possible resistance mechanism, and the depletion of MERTK with shRNA enhanced the cytotoxic effect of temozolomide and carboplatin.[74] During the course of our studies, the development and clinical use of foretinib were discontinued, so we compared it with the clinically relevant receptor tyrosine kinase inhibitor cabozantinib, essentially inhibiting the same receptor tyrosine kinases. Because the in vitro results were very promising, the combination of trabectedin with cabozantinib was used in the in vivo experiments.

As mentioned before, we observed a substantial antitumor effect of trabectedin, with an overall response rate of 47%, and monotreatment by cabozantinib essentially completely blocked the further growth of tumors with an overall response rate of almost 100%. However, trabectedin did not enhance the effect of monotreatment by cabozantinib. This finding was somewhat disappointing, but it could be explained by the strong effect of cabozantinib treatment and the fact that trabectedin can only be administered once a week due to its toxicity profile. Possibly, if cabozantinib by itself almost fully blocks cell proliferation, then trabectedin would not have any additional effect. Also, in vitro in most cell lines, the highest concentration of cabozantinib showed no or very limited synergism with trabectedin. Therefore, we still believe that the combination of trabectedin with cabozantinib or, even better, a more specific MERTK inhibitor is a therapeutic option for patients with metastatic UM, because in the immunocompromised mouse models the effect of trabectedin on the immune microenvironment was not taken into account. In this respect, it is interesting to note that more specific MERTK or MERTK/AXL double inhibitors are being tested in clinical trials.[75] Importantly, MERTK not only has cell-intrinsic proliferative and survival functions but also creates an immunosuppressive environment, the inhibition of which might sensitize metastatic UM for immunotherapy. In line with that, the recent findings suggest a mechanistic link between genetic aberrations in UM and activity of MERTK in tumor-associated macrophages. According to Kaler et al.,[76] BAP1 loss results in upregulation of a ligand and agonist of MERTK, PROS1, in UM cells through epigenetic mechanisms. In turn, membrane-bound PROS1 on tumor cells interacts with MERTK on nearby macrophages, leading to phosphorylation of MERTK and activation of downstream signaling that promotes M2 polarization. PROS1 shares structural and functional similarities with GAS6.[77,78] According to our analysis of the clinical datasets described earlier, GAS6 expression is, similar to PROS1, correlated with BAP1 expression, and it might have the same effects on the tumor microenvironment. Therefore, we would be very interested in seeing a clinical trial for patients with UM metastatic that combines trabectedin with currently tested MERTK/AXL inhibitor(s).

Acknowledgments

The authors thank Marco Herold for the gift of the lentiviral vectors to make inducible shRNA expression vectors, Emilie Vinolo for managing the UM CURE project, and the animal platform of the Institut Curie.

Supported by a grant from the European Union's Horizon 2020 project "UM Cure 2020" (667787).

Disclosure: **K. Glinkina**, None; **F. Nemati**, None; **A.F.A.S. Teunisse**, None; **M.C. Gelmi**, None; **V. Etienne**, None; **M.J. Kuipers**, None; **S. Alsafadi**, None; **M.J. Jager**, None; **D. Decaudin**, None; **A.G. Jochemsen**, None

References

1. Virgili G, Gatta G, Ciccolallo L, et al. Incidence of uveal melanoma in Europe. *Ophthalmology*. 2007;114(12):2309–2315.
2. Koutsandrea C, Moschos MM, Dimissianos M, Georgopoulos G, Ladas I, Apostolopoulos M. Metastasis rates and sites after treatment for choroidal melanoma by proton beam irradiation or by enucleation. *Clin Ophthalmol*. 2008;2(4):989–995.
3. Diener-West M, Reynolds SM, Agugliaro DJ, et al. Screening for metastasis from choroidal melanoma: the Collaborative Ocular Melanoma Study Group Report 23. *J Clin Oncol*. 2004;22(12):2438–2444.
4. Alexander HR, Libutti SK, Pingpank JF, et al. Hyperthermic isolated hepatic perfusion using melphalan for patients with ocular melanoma metastatic to liver. *Clin Cancer Res*. 2003;9(17):6343–6349.
5. Noter SL, Rothbarth J, Pijl MEJ, et al. Isolated hepatic perfusion with high-dose melphalan for the treatment of uveal melanoma metastases confined to the liver. *Melanoma Res*. 2004;14(1):67–72.
6. Meijer TS, Burgmans MC, de Leede EM, et al. Percutaneous hepatic perfusion with melphalan in patients with unresectable ocular melanoma metastases confined to the liver: a prospective phase II study. *Ann Surg Oncol*. 2021;28(2):1130–1141.
7. Dewald CLA, Warnke MM, Bruening R, et al. Percutaneous hepatic perfusion (PHP) with melphalan in liver-dominant metastatic uveal melanoma: the German experience. *Cancers*. 2021;14(1):118.
8. Yang J, Manson DK, Marr BP, Carvajal RD. Treatment of uveal melanoma: where are we now? *Adv Med Oncol*. 2018;10:1758834018757175.
9. Carvajal RD, Piperno-Neumann S, Kapiteijn E, et al. Selumetinib in combination with dacarbazine in patients with metastatic uveal melanoma: a phase III, multicenter, randomized trial (SUMIT). *J Clin Oncol*. 2018;36(12):1232–1239.
10. Spagnolo F, Grosso M, Picasso V, Tornari E, Pesce M, Quierolo P. Treatment of metastatic uveal melanoma with intravenous fotemustine. *Melanoma Res*. 2013;23(3):196–198.
11. Falchook GS, Lewis KD, Infante JR, et al. Activity of the oral MEK inhibitor trametinib in patients with advanced melanoma: a phase 1 dose-escalation trial. *Lancet Oncol*. 2012;13(8):782–789.
12. Penel N, Delcambre C, Durando X, et al. O-Mel-Inib: a Cancéro-pôle Nord-Ouest multicenter phase II trial of high-dose imatinib mesylate in metastatic uveal melanoma. *Invest New Drug*. 2008;26(6):561–565.
13. Shah S, Luke JJ, Jacene HA, et al. Results from phase II trial of HSP90 inhibitor, STA-9090 (ganetespib), in metastatic uveal melanoma. *Melanoma Res*. 2018;28(6):605–610.

14. Rossi E, Pagliara MM, Orteschi D, et al. Pembrolizumab as first-line treatment for metastatic uveal melanoma. *Cancer Immunol Immun*. 2019;68(7):1179–1185.
15. Rodrigues M, Mobuchon L, Houy A, et al. Outlier response to anti-PD1 in uveal melanoma reveals germline MBD4 mutations in hypermutated tumors. *Nat Commun*. 2018;9(1):1866.
16. Nathan P, Hassel JC, Rutkowski P, et al. Overall survival benefit with Tebentafusp in metastatic uveal melanoma. *N Engl J Med*. 2021;385(13):1196–1206.
17. Johansson PA, Brooks K, Newell F, et al. Whole genome landscapes of uveal melanoma show an ultraviolet radiation signature in iris tumours. *Nat Commun*. 2020;11(1):2408.
18. Yarchoan M, Hopkins A, Jaffee EM. Tumor mutational burden and response rate to PD-1 inhibition. *N Engl J Med*. 2017;377(25):2500–2501.
19. Robertson AG, Shih J, Yau C, et al. Integrative analysis identifies four molecular and clinical subsets in uveal melanoma. *Cancer Cell*. 2018;32(2):204–220.
20. Johansson P, Aoude LG, Wadt K, et al. Deep sequencing of uveal melanoma identifies a recurrent mutation in PLCB4. *Oncotarget*. 2016;7(4):4624–4631.
21. Moore AR, Ceraudo E, Sher JJ, et al. Recurrent activating mutations of G-protein-coupled receptor CYSLTR2 in uveal melanoma. *Nat Genet*. 2016;48(6):675–680.
22. Chen X, Wu QX, Depeille P, et al. RasGRP3 mediates MAPK pathway activation in GNAQ mutant uveal melanoma. *Cancer Cell*. 2017;31(5):685–696.
23. Yu FX, Luo J, Mo JS, et al. Mutant Gq/11 promote uveal melanoma tumorigenesis by activating YAP. *Cancer Cell*. 2014;25(6):822–830.
24. Aalto Y, Eriksson L, Seregard S, Larsson O, Knuutila S. Concomitant loss of chromosome 3 and whole arm losses and gains of chromosome 1, 6, or 8 in metastasizing primary uveal melanoma. *Invest Ophthalmol Vis Sci*. 2001;42(2):313–317.
25. Sisley K, Rennie IG, Parsons MA, et al. Abnormalities of chromosomes 3 and 8 in posterior uveal melanoma correlate with prognosis. *Genes Chromosomes Cancer*. 1997;19(1):22–28.
26. Damato B, Dopierala JA, Coupland SE. Genotypic profiling of 452 choroidal melanomas with multiplex ligation-dependent probe amplification. *Clin Cancer Res*. 2010;16(24):6083–6092.
27. Ewens KG, Kanetsky PA, Richards-Yutz J, et al. Genomic profile of 320 uveal melanoma cases: chromosome 8p-loss and metastatic outcome. *Invest Ophthalmol Vis Sci*. 2013;54(8):5721–5729.
28. Harbour JW, Onken MD, Roberson EDO, et al. Frequent mutation of BAP1 in metastasizing uveal melanomas. *Science*. 2010;330(6009):1410–1413.
29. Martin M, Masshofer L, Temming P, et al. Exome sequencing identifies recurrent somatic mutations in EIF1AX and SF3B1 in uveal melanoma with disomy 3. *Nat Genet*. 2013;45(8):933–936.
30. Onken MD, Makepeace CM, Kaltenbronn KM, et al. Targeting primary and metastatic uveal melanoma with a G protein inhibitor. *J Biol Chem*. 2021;296:100403.
31. de Lange J, Teunisse AFAS, Verlaan-de Vries M, et al. High levels of Hdmx promote cell growth in a subset of uveal melanomas. *Am J Cancer Res*. 2012;2(5):492–507.
32. Harbour JW, Roberson EDO, Anbunathan H, Onken MD, Worley LA, Bowcock AM. Recurrent mutations at codon 625 of the splicing factor SF3B1 in uveal melanoma. *Nat Genet*. 2013;45(2):133–135.
33. Furney SJ, Pedersen M, Gentien D, et al. SF3B1 mutations are associated with alternative splicing in uveal melanoma. *Cancer Discov*. 2013;3(10):1122–1129.
34. Mallikarjuna K, Pushparaj V, Biswas J, Krishnakumar S. Expression of epidermal growth factor receptor, ezrin, hepatocyte growth factor, and c-Met in uveal melanoma: an immunohistochemical study. *Curr Eye Res*. 2007;32(3):281–290.
35. van Ginkel PR, Gee RL, Shearer RL, et al. Expression of the receptor tyrosine kinase Axl promotes ocular melanoma cell survival. *Cancer Res*. 2004;64(1):128–134.
36. Monk BJ, Herzog TJ, Wang G, et al. A phase 3 randomized, open-label, multicenter trial for safety and efficacy of combined trabectedin and pegylated liposomal doxorubicin therapy for recurrent ovarian cancer. *Gynecol Oncol*. 2020;156(3):535–544.
37. Borad MJ, Bai LY, Chen MH, et al. Silmitasertib (CX-4945) in combination with gemcitabine and cisplatin as first-line treatment for patients with locally advanced or metastatic cholangiocarcinoma: a phase Ib/II study. *J Clin Oncol*. 2021;39(3):312–312.
38. Rayson D, Lupichuk S, Potvin K, et al. Canadian Cancer Trials Group IND197: a phase II study of foretinib in patients with estrogen receptor, progesterone receptor, and human epidermal growth factor receptor 2-negative recurrent or metastatic breast cancer. *Breast Cancer Res Treat*. 2016;157(1):109–116.
39. Andreeff M, Kelly KR, Yee K, et al. Results of the phase I trial of RG7112, a small-molecule MDM2 antagonist in leukemia. *Clin Cancer Res*. 2016;22(4):868–876.
40. Luyten GPM, Naus NC, Mooy CM, et al. Establishment and characterization of primary and metastatic uveal melanoma cell lines. *Int J Cancer*. 1996;66(3):380–387.
41. Amirouchene-Angelozzi N, Nemati F, Gentien D, et al. Establishment of novel cell lines recapitulating the genetic landscape of uveal melanoma and preclinical validation of mTOR as a therapeutic target. *Mol Oncol*. 2014;8(8):1508–1520.
42. Herold MJ, van den Brandt J, Seibler J, Reichardt HM. Inducible and reversible gene silencing by stable integration of an shRNA-encoding lentivirus in transgenic rats. *Proc Natl Acad Sci USA*. 2008;105(47):18507–18512.
43. Heijkants RC, Nieveen M, 't Hart KC, Teunisse AFAS, Jochemsen AG. Targeting MDMX and PKC delta to improve current uveal melanoma therapeutic strategies. *Oncogenesis*. 2018;7(3):33.
44. Carlotti F, Bazuine M, Kekarainen T, et al. Lentiviral vectors efficiently transduce quiescent mature 3T3-L1 adipocytes. *Mol Ther*. 2004;9(2):209–217.
45. Bliss CI. Calculation of microbial assays. *Bacteriol Rev*. 1956;20(4):243–258.
46. Fitzgerald JB, Schoeberl B, Nielsen UB, Sorger PK. Systems biology and combination therapy in the quest for clinical efficacy. *Nat Chem Biol*. 2006;2(9):458–466.
47. Gao H, Korn JM, Ferretti S, et al. High-throughput screening using patient-derived tumor xenografts to predict clinical trial drug response. *Nat Med*. 2015;21(11):1318–1325.
48. Robertson AG, Shih J, Yau C, et al. Integrative analysis identifies four molecular and clinical subsets in uveal melanoma. *Cancer Cell*. 2018;32(2):204–220.
49. Di Maira G, Salvi M, Arrigoni G, et al. Protein kinase CK2 phosphorylates and upregulates Akt/PKB. *Cell Death Differ*. 2005;12(6):668–677.
50. Kim H, Choi K, Kang H, et al. Identification of a novel function of CX-4945 as a splicing regulator. *PLoS One*. 2014;9(4):e94978.
51. Dewaele M, Tabaglio T, Willekens K, et al. Antisense oligonucleotide-mediated MDM4 exon 6 skipping impairs tumor growth. *J Clin Invest*. 2016;126(1):68–84.
52. Erba E, Bergamaschi D, Bassano L, et al. Ecteinascidin-743 (ET-743), a natural marine compound, with a unique mechanism of action. *Eur J Cancer*. 2001;37(1):97–105.

Investigative Ophthalmology & Visual Science

53. Soares DG, Escargueil AE, Poindessous V, et al. Replication and homologous recombination repair regulate DNA double-strand break formation by the antitumor alkylator ecteinascidin 743. *Proc Natl Acad Sci USA*. 2007;104(32):13062–13067.
54. Gao JJ, Aksoy BA, Dogrusoz U, et al. Integrative analysis of complex cancer genomics and clinical profiles using the cBioPortal. *Sci Signal*. 2013;6(269):pl1.
55. Cerami E, Gao JJ, Dogrusoz U, et al. The cBio Cancer Genomics Portal: an open platform for exploring multidimensional cancer genomics data. *Cancer Discov*. 2012;2(5):401–404.
56. Choueiri TK, Powles T, Burotto M, et al. Nivolumab plus cabozantinib versus sunitinib for advanced renal-cell carcinoma. *N Engl J Med*. 2021;384(9):829–841.
57. Luke JJ, Olson DJ, Allred JB, et al. Randomized phase II trial and tumor mutational spectrum analysis from cabozantinib versus chemotherapy in metastatic uveal melanoma (Alliance A091201). *Clin Cancer Res*. 2020;26(4):804–811.
58. Schmittel A, Scheulen ME, Bechrakis NE, et al. Phase II trial of cisplatin, gemcitabine and treosulfan in patients with metastatic uveal melanoma. *Melanoma Res*. 2005;15(3):205–207.
59. Schinzari G, Rossi E, Cassano A, et al. Cisplatin, dacarbazine and vinblastine as first line chemotherapy for liver metastatic uveal melanoma in the era of immunotherapy: a single institution phase II study. *Melanoma Res*. 2017;27(6):591–595.
60. O'Neill PA, Butt M, Eswar CV, Gillis P, Marshall E. A prospective single arm phase II study of dacarbazine and treosulfan as first-line therapy in metastatic uveal melanoma. *Melanoma Res*. 2006;16(3):245–248.
61. Kivela T, Suciu S, Hansson J, et al. Bleomycin, vincristine, lomustine and dacarbazine (BOLD) in combination with recombinant interferon alpha-2b for metastatic uveal melanoma. *Eur J Cancer*. 2003;39(8):1115–1120.
62. D'Incalci M, Badri N, Galmarini CM, Allavena P. Trabectedin, a drug acting on both cancer cells and the tumour microenvironment. *Br J Cancer*. 2014;111(4):646–650.
63. Ratti C, Botti L, Cancila V, et al. Trabectedin overrides osteosarcoma differentiative block and reprograms the tumor immune environment enabling effective combination with immune checkpoint inhibitors. *Clin Cancer Res*. 2017;23(17):5149–5161.
64. Demetri GD, von Mehren M, Jones RL, et al. Efficacy and safety of trabectedin or dacarbazine for metastatic liposarcoma or leiomyosarcoma after failure of conventional chemotherapy: results of a phase III randomized multicenter clinical trial. *J Clin Oncol*. 2016;34(8):786–793.
65. Vidal L, Magem M, Barlow C, et al. Phase I clinical and pharmacokinetic study of trabectedin and carboplatin in patients with advanced solid tumors. *Invest New Drug*. 2012;30(2):616–628.
66. Meggio F, Marin O, Pinna LA. Substrate specificity of protein kinase CK2. *Cell Mol Biol Res*. 1994;40(5-6):401–409.
67. Meggio F, Pinna LA. One-thousand-and-one substrates of protein kinase CK2? *FASEB J*. 2003;17(3):349–368.
68. D'Amore C, Borgo C, Sarno S, Salvi M. Role of CK2 inhibitor CX-4945 in anti-cancer combination therapy – potential clinical relevance. *Cell Oncol*. 2020;43(6):1003–1016.
69. Martin M, Masshofer L, Temming P, et al. Exome sequencing identifies recurrent somatic mutations in EIF1AX and SF3B1 in uveal melanoma with disomy 3. *Nat Genet*. 2013;45(8):933–936.
70. Surriga O, Rajasekhar VK, Ambrosini G, Dogan Y, Huang R, Schwartz GK. Crizotinib, a c-MET inhibitor, prevents metastasis in a metastatic uveal melanoma model. *Mol Cancer Ther*. 2013;12(12):2817–2826.
71. Gardner FP, Serie DJ, Salomao DR, et al. c-MET expression in primary and liver metastases in uveal melanoma. *Melanoma Res*. 2014;24(6):617–620.
72. Knubel KH, Pernu BM, Sufit A, Nelson S, Pierce AM, Keating AK. MerTK inhibition is a novel therapeutic approach for glioblastoma multiforme. *Oncotarget*. 2014;5(5):1338–1351.
73. Sufit A, Lee-Sherick AB, DeRyckere D, et al. MERTK inhibition induces polyploidy and promotes cell death and cellular senescence in glioblastoma multiforme. *PLoS One*. 2016;11:e0165107.
74. Keating AK, Kim GK, Jones AE, et al. Inhibition of Mer and Axl receptor tyrosine kinases in astrocytoma cells leads to Increased apoptosis and improved chemosensitivity. *Mol Cancer Ther*. 2010;9(5):1298–1307.
75. Huelse JM, Fridlyand DM, Earp S, DeRyckere D, Graham DK. MERTK in cancer therapy: targeting the receptor tyrosine kinase in tumor cells and the immune system. *Pharmacol Ther*. 2020;213:107577.
76. Kaler CJ, Dollar JJ, Cruz AM, et al. BAP1 loss promotes suppressive tumor immune microenvironment via upregulation of PROS1 in class 2 uveal melanomas. *Cancers (Basel)*. 2022;14(15):3678.
77. Hafizi S, Dahlback B. Gas6 and protein S: vitamin K-dependent ligands for the Axl receptor tyrosine kinase subfamily. *FEBS J*. 2006;273(23):5231–5244.
78. Laurance S, Lemarie CA, Blostein MD. Growth arrest-specific gene 6 (gas6) and vascular hemostasis. *Adv Nutr*. 2012;3(2):196–203.

Investigative Ophthalmology & Visual Science